Dear Author,

Please, note that changes made to the HTML content will be added to the article before publication, but are not reflected in this PDF.

Note also that this file should not be used for submitting corrections.

Science of the Total Environment xxx (2015) xxx–xxx

Contents lists available at ScienceDirect

Science of the Total Environment

journal homepage: www.elsevier.com/locate/scitotenv

# High field FT-ICR mass spectrometry for molecular characterization of snow board from Moscow regions

Dmitry M. Mazur [a,1], Mourad Harir [b,c,1], Philippe Schmitt-Kopplin [b,c,*], Olga V. Polyakova [a], Albert T. Lebedev [a,**]

[a] Organic Chemistry Department, M.V. Lomonosov Moscow State University, 119991, Leninskie Gori, 1, bld. 3, Moscow, Russia
[b] Helmholtz Zentrum Muenchen, German Research Center for Environmental Health, Research Unit Analytical Biogeochemistry (BGC), Ingolstaedter Landstrasse 1, D-85764, Neuherberg, Germany
[c] Chair of Analytical Food Chemistry, Technische Universität München, Freising-Weihenstephan, Germany

## HIGHLIGHTS

- High field FT-ICR mass spectrometry was used to study air pollution in Moscow.
- More than 2000 elemental compositions of pollutants were found in snow samples.
- The statistical processing allowed clustering the results into 3 groups.
- The possible sources of various groups of pollutants were proposed.

## GRAPHICAL ABSTRACT

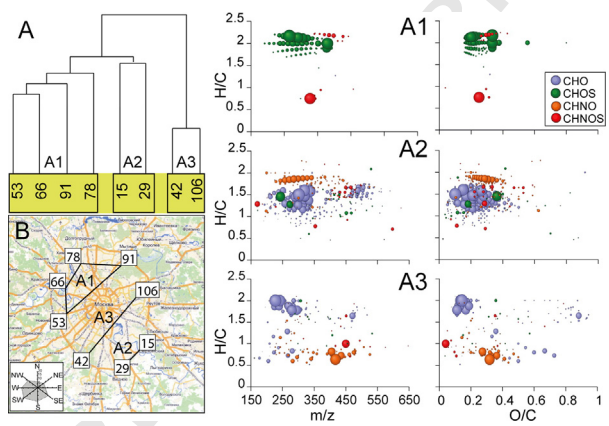


## ARTICLE INFO

*Article history:*
Received 3 October 2015
Received in revised form 17 February 2016
Accepted 25 February 2016
Available online xxxx

Editor: D. Barcelo

*Keywords:*
Snow boards
Moscow region
FT-ICR-MS
HCA
Molecular compositions
Air pollution

## ABSTRACT

High field Fourier transform ion cyclotron resonance (FT-ICR) mass spectrometry analysis of eight snow samples from Moscow city allowed us to identify more than 2000 various elemental compositions corresponding to regional air pollutants. The hierarchical cluster analyses (HCA) of the data showed good concordance of three main groups of samples with the main wind directions. The North-West group (A1) is represented by several homologous CHOS series of aliphatic organic aerosols. They may form as a result of enhanced photochemical reactions including oxidation of hydrocarbons with sulfonations due to higher amount of $SO_2$ emissions in the atmosphere in this region. Group A2, corresponding to the South-East part of Moscow, contains large amount of oxidized hydrocarbons of different sources that may form during oxidation in atmosphere. These hydrocarbons appear correlated to emissions from traffic, neighboring oil refinery, and power plants. Another family of compounds specific for this region involves CHNO substances formed during oxidation processes including $NO_x$ and $NO_3$ radical since emissions of $NO_x$ are higher in this part of the city. Group A3 is rich in CHO type of compounds with high H/C and low O/C ratios, which is characteristic of oxidized hydrocarbon-like organic aerosol. CHNO types of compounds in A3 group are probably nitro derivatives of condensed hydrocarbons

* Correspondence to: Ph. Schmitt-Kopplin, Helmholtz Zentrum Muenchen, German Research Center for Environmental Health, Research Unit Analytical Biogeochemistry (BGC), Ingolstaedter Landstrasse 1, D-85764 Neuherberg, Germany.
** Corresponding author.
*E-mail addresses:* schmitt-kopplin@helmholtz-muenchen.de (P. Schmitt-Kopplin), a.lebedev@org.chem.msu.ru (A.T. Lebedev).
[1] Contributed equally to the work.

http://dx.doi.org/10.1016/j.scitotenv.2016.02.178
0048-9697/© 2015 Published by Elsevier B.V.

such as PAH. This non-targeted profiling revealed site specific distribution of pollutants and gives a chance to develop new strategies in air quality control and further studies of Moscow environment.



## 1. Introduction

Human health is highly influenced by environmental factors. Among them air quality highly affects people's breath inducing lung related diseases. Air, as composed of the gaseous part and various aerosols and dust particles can have either positive or negative effect on human health. Therefore it is essential to setup air quality criteria and monitor these, especially in cities and highly populated areas. Air quality control is especially important as preventions in industrialized areas.

Besides several classical approaches to study atmospheric pollution, the analysis of snow represents a very efficient approach of passive sampling, especially in the regions with cold climate or in the highlands (Laniewski et al., 1998; Lebedev et al., 1998; Lebedev et al., 2003; Poliakova et al., 2003; Fries et al., 2007; Zoccolillo et al., 2007; Sieg et al., 2008; Fries et al., 2008; Polyakova et al., 2012). The available results of air pollution using snow core were reviewed in recent publication (Lebedev et al., 2015). Snow is an excellent preserving matrix, which can capture and hold both polar and non-polar compounds. Due to low temperature even rather unstable compounds (e.g. phenols) can be quenched in the snow matrix for longer times. It is also very convenient matrix for sample preparation, as it can be treated the same as water, i.e. using with the well-established various standard extraction techniques. Analysis of snow can be performed at once as it fell down or after some time as passive sampling. The analysis of the whole snow layer at the end of the winter period provides a good estimation of the long term atmospheric pollution.

Within targeted or non-targeted environmental analysis, mass spectrometry represents the best analytical tool combining selectivity, sensitivity, reliability, and information capacity (Lebedev, 2013). Nevertheless when considering all the available data on the snow analysis it becomes clear that GC/MS combined with electron ionization (EI) was used for this purpose almost exclusively (Lebedev et al., 2015). This classical approach profit of existing databases and gives a lot of information regarding small volatile as well as semi volatile organic molecules, many of which became of major concern from the environmental point of view (PAH, BTEX, organochlorines, phthalates, PCB, etc.). GC/MS or GC × GC/MS identification of the knowns and structural elucidation of the unknowns may be considerably more reliable if accompanied by accurate mass measurements (Lebedev et al., 2013).

Nevertheless to deal with polar and nonvolatile substances in snow samples (as in any others) it is better to use electrospray (ESI) or atmospheric pressure chemical ionization (APCI) rather than EI. In this field FT-ICR mass spectrometry coupled to ESI ion source can provide ultrahigh resolution and mass accuracy making it a unique analytical tool for the screening of complex mixtures with several thousands of components. The application of ESI provides only protonated (deprotonated) molecules, while accurate mass measurements reliably establish elemental composition of each component. The data obtained that way may be used to compare different pools of samples. Definitely in the case of snow samples they allow making some insights to understand the processes in atmosphere depending on the conditions.

High field FT-ICR-MS was shown previously as the most useful analytical tool to identify atmospheric organic matter (AOM) and dissolved organic matter (DOM) (Schmitt-Kopplin et al. 2010; Nizkorodov et al., 2011; Zhao et al., 2013). Recently, high field FT-ICR-MS was applied to examine organic matter in Antarctic snow (Antony et al., 2014). Nowadays there is no list of priority pollutants for Moscow regions. Therefore the most relevant compounds specific for a highly industrial and populated megacity as Moscow remain unknown. To propose a list of priority pollutants for Moscow, we have recently carried out GC-MS and ICP-MS studies (Polyakova et al., 2012). To extend this study and to get a wider list of compounds present in the Moscow air we used herein high field FT-ICR-MS to screen snow samples from various regions in Moscow. Having knowledge of a complete set of the pollutants of various chemistry it becomes possible to arrange environmental protection measures and identify the most dangerous sources of air pollution.

## 2. Materials and methods

### 2.1. Sampling and weather conditions

Eight samples of snow were collected along the perimeter (109 km) of the Moscow belt road in March 2013. The samples were collected in 25–100 m from the road in the following points: 15, 29, 42, 53, 66, 78, 91 and 106 km. The height of snow layer in sampling points was between 35 and 50 cm. The winter of 2012–2013 was longer than usual — 127 days of snow cover. Mean temperature during winter months (end of November — end of March) was about −7 °C, though some days frosts were down to −25 °C. According to meteorological data only 20% of all winter days were clear. The total amount of precipitation during this period was about 150 cm, with record height of snow layer in the end of March — 77 cm. Stability of snow cover was extremely long — 142 days. The sampling was carried out with a 10 cm diameter pipe. The snow was placed in 3 liter glass jars and melted at room temperature. Melted water was then filtrated through the paper filters. The water samples were diluted with methanol (LC-MS CHROMASOLV, Fluka) 1:1 and injected directly into ESI source.

### 2.2. FT-ICR-MS analysis

Ultrahigh-resolution Fourier transform ion cyclotron mass spectra (FT-ICR-MS) were acquired using a 12 T Bruker Solarix mass spectrometer (Bruker Daltonics, Bremen, Germany) fitted with an electrospray ionization source in negative mode. Diluted snow samples in methanol were injected into the electrospray source using a micro-liter pump at a flow rate of 120 μL/h with a nebulizer gas pressure of 138 kPa and a drying gas pressure of 103 kPa. A source heater temperature of 200 °C was maintained to ensure rapid desolvation in the ionized droplets. Spectra were first externally calibrated on clusters of arginine in MeOH (0.57 μmol/L) and internal calibration was systematically done in the presence of natural organic matter reaching accuracy values lower than 500 ppb. The spectra were acquired with a time domain of 4 megawords and 500 scans were accumulated for each mass spectrum. Calculation of elemental formulas for each peak was done in a batch mode by an in-house written software tool.

### 2.3. Molecular formula assignments

The generated formulae were validated by setting sensible chemical constraints [N rule, O/C ratio ≤ 1. H/C ratio ≤ 2n + 2 ($C_nH_{2n+2}$). Element counts: C ≤ 100, H ≤ 200, O ≤ 80, N ≤ 3, S ≤ 2 and mass accuracy window (set at 500 ppb)]. Final formulae were generated and categorized into groups containing CHO, CHNO, CHOS or CHNOS molecular compositions which were used to reconstruct the group-selective mass spectra (Schmitt-Kopplin et al. 2010). The similarities (or dissimilarities) among the snow samples were investigated using hierarchical cluster analysis (HCA). The cluster analysis was performed using Pearson correlation and only on mass peaks that had unambiguously assigned molecular formulas. A comprehensive list of data including masses



Please cite this article as: Mazur, D.M., et al., High field FT-ICR mass spectrometry for molecular characterization of snow board from Moscow regions, Sci Total Environ (2015), http://dx.doi.org/10.1016/j.scitotenv.2016.02.178

and intensities from all spectra was provided in a multidimensional data set. By using this approach, the mass distribution and intensities are reflected in statistical calculations. The proportions of peaks abundance in each class of samples are studied using van Krevelen plots, Kendrick mass defect (KMD), double bond equivalent (DBE) and the average carbon oxidation state. These indices are reported in details elsewhere (Van Krevelen, 1950; Headley et al., 2007, 2010; Hertkorn et al., 2008; Schmitt-Kopplin et al., 2010a, 2010b, Kroll et al., 2011; Cottrell et al., 2013; Ortiz et al., 2014; Yassine et al., 2012, 2014).

## 3. Results and discussion

### 3.1. FT-ICR mass spectra

The atmospheric pollution of the Moscow region has never been studied thoroughly. Therefore the present results are quite important to understand the specificity of composition of aerosols and atmospheric processes occurred in winter season. High field FT-ICR-MS provides ultrahigh resolution and mass accuracy allowing the profiling of compounds on the CHNOS compositional space. Over 2000 elemental compositions were identified for each of the 8 snow samples out of thousands of signals in electrospray negative ionization flow injection FT-ICR-MS. As far as the sample preparation was maximally reduced we can consider that the losses during sampling and sample preparation were minimal. At the first glance, the mass spectra of all the samples look very similar showing typical distribution of negative ion signals and covering *m/z* range from 130 to 700 Da (Fig. 1A). Presentation of such large amount of data is illustrated through van Krevelen plots and Kendrick mass defect as most effective tools to extract maximal information about chemical composition in most complex organic matter (Hertkorn et al., 2007; Hertkorn et al., 2008; Schmitt-Kopplin et al. 2010). Mass resolved atomic H/C ratio and van Krevelen plots of typical snow sample from Moscow (Fig. 1B,C) show that the spectrum is saturated with different types of chemical compositions. Considering the classification of organic matter in van Krevelen plot we can distinguish atmospheric primary organic aerosols (POA), atmospheric secondary organic aerosols (SOA), terrestrial natural organic matter and sulfonated SOA. General data on elemental composition of each sample is presented in Table 1. The average number of C atoms in all the samples is concentrated in relatively narrow range between 16 and 18 atoms. The majority of substances have H/C ratio more than 1 and O/C ration <0.5.

The proportion of O atoms in each composition is relatively similar with about 5 atoms. The average value of S atoms in first 4 samples (53, 66, 91, and 78) is higher as compared with the other samples. This also is validated using $C/S_{avrg}$ ratio with lower values for the mentioned samples (Table 1). Accordingly, the computed average values of the double bond equivalent (DBE) as well as mass-to-charge (*m/z*) cover ranges between 4 and 6 and 310–341 Da, respectively. Though each sample represents a distinct point in Moscow with contribution of some specific substances depending on the pollution sources, it becomes very laborious to discuss every sample separately and describe their chemical compositions. Thus, it is more efficient to analyze this massive data array using statistical evaluation. The shared molecular compositions in all eight samples thereby were not discussed, regarding them as natural organic matter background.

### 3.2. Clustering analysis properties

Classification of the FT-ICR mass spectra data sets of the eight snow samples was assessed using hierarchical cluster analysis (HCA) based on the unequivocally assigned molecular compositions and their corresponding intensities data(Fig. 2A). The HCA allowed grouping the eight snow samples into three main groups — A1, A2, A3 (Fig. 2A,B). This would be used to extract the relative abundance of compounds in each group of samples. Taking into account the wind direction in Moscow region, we can emphasize that these three groups correlate well with the dominant winds in the city of South West and South.

In addition, detailed analysis of specific elemental compositions for each group of samples is shown in Fig. 2A1, A2 and A3. The van Krevelen plots show that different types of compounds are characteristic for each of the three groups. The size of each bubble indicates the ions peaks intensities. Group A1 stands out with specific CHOS and CHNOS molecular series while group A2 with various classes of CHO and CHNO molecular series. Group A3 is totally different from groups A1 and A2 with distinct CHO and CHNO molecular series. Discussion of each group is presented separately in the next sections.

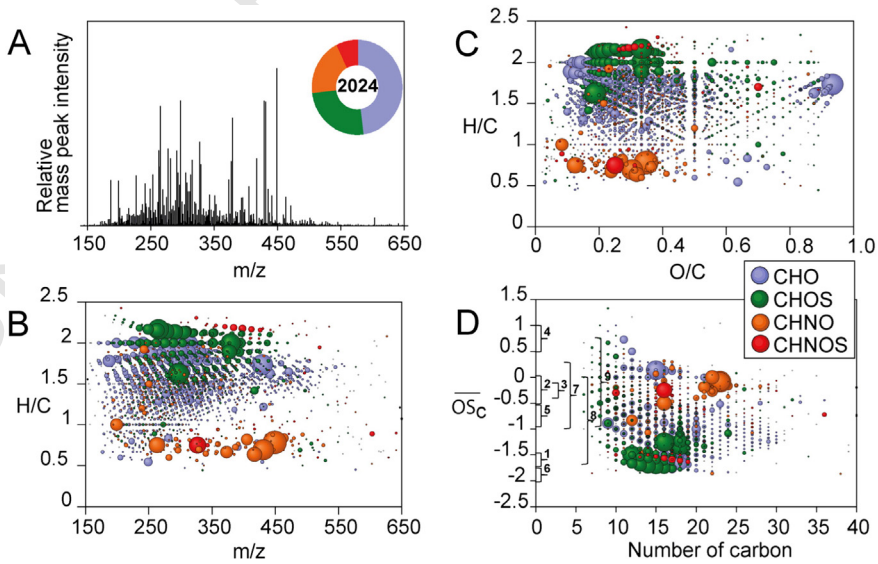


**Fig. 1.** (A) Negative electrospray FT-ICR mass spectrum of the snow sample (53). (B) and (C) represent the H/C versus *m/z* (middle) and H/C versus O/C van Krevelen plot of CHO (blue), CHNO (orange), CHOS (green) and CHONS (red) molecular series. (D) Carbon oxidation state versus number of carbon: Overlays of compound classes designate organic aerosol classes for carbon oxidation state as: (1) hydrocarbon-like organic aerosol (HOA), (2) semi-volatile oxygenated organic aerosol (SV OOA), (3) humic-like substances (HULIS), (4) low volatility oxygenated organic aerosol (LV-OOA), (5) water soluble organic carbon (WSOC), (6) vehicle exhaust, (7) biogenic aerosol, (8) anthropogenic, and (9) aged aerosol and biomass burning organic aerosol (BBOA) (Kroll et al., 2011, Cottrell et al., 2013). (For interpretation of the references to color in this figure legend, the reader is referred to the web version of this article.)

Please cite this article as: Mazur, D.M., et al., High field FT-ICR mass spectrometry for molecular characterization of snow board from Moscow regions, Sci Total Environ (2015), http://dx.doi.org/10.1016/j.scitotenv.2016.02.178

**Table 1**
Computed average values of carbon oxidation state, C, H, N, O, S, O/C, H/C, C/S, C/N, DBE and mass-to-charge ($m/z$) based upon intensity-weighted averages of mass peaks as generated in mass spectra of snow samples.

| Snow samples | $OS_{c\ avrg}$ | $C_{avrg}$ | $H_{avrg}$ | $N_{avrg}$ | $O_{avrg}$ | $S_{avrg}$ | $O/C_{avrg}$ | $H/C_{avrg}$ | $C/S_{avrg}$ | $C/N_{avrg}$ | $DBE_{avrg}$ | $m/z_{avrg}$ |
|---|---|---|---|---|---|---|---|---|---|---|---|---|
| 53 | −0.92 | 16.35 | 25.39 | 0.32 | 5.14 | 0.37 | 0.31 | 1.55 | 44.14 | 51.10 | 4.82 | 319.36 |
| 66 | −1.08 | 16.75 | 27.08 | 0.23 | 4.43 | 0.39 | 0.26 | 1.62 | 42.95 | 73.70 | 4.32 | 313.78 |
| 91 | −1.04 | 16.34 | 26.62 | 0.17 | 4.61 | 0.42 | 0.28 | 1.63 | 38.93 | 96.10 | 4.11 | 311.36 |
| 78 | −1.03 | 16.29 | 26.62 | 0.22 | 4.85 | 0.42 | 0.30 | 1.63 | 38.60 | 72.84 | 4.09 | 315.59 |
| 15 | −0.83 | 16.11 | 23.96 | 0.35 | 5.01 | 0.27 | 0.31 | 1.49 | 60.03 | 46.15 | 5.31 | 310.02 |
| 29 | −0.89 | 17.51 | 25.83 | 0.41 | 5.10 | 0.37 | 0.29 | 1.48 | 47.61 | 42.45 | 5.80 | 334.29 |
| 42 | −0.96 | 17.93 | 27.28 | 0.28 | 5.01 | 0.22 | 0.28 | 1.52 | 82.37 | 63.75 | 5.42 | 332.62 |
| 106 | −0.93 | 18.26 | 27.85 | 0.34 | 5.25 | 0.20 | 0.29 | 1.53 | 91.93 | 53.93 | 5.51 | 341.17 |

### 3.3. Compound class assignment

#### 3.3.1. Group A1

As shown in Fig. 2, group A1 consists essentially of CHOS type of compounds in comparison with groups A2 and A3. Beside this, group A1 have rather high H/C ratio with mean value 1.93 ± 0.22, relatively low O/C ratio with mean value 0.25 ± 0.09 (mean value ± standard deviation), low DBE (0–3) and average carbon oxidation state (OSc) between −1.25 and −1.75. These elemental ratios and OSc are typical for hydrocarbon-like organic aerosol and vehicle exhaust compounds, i.e. aliphatic sulfate esters or other S-oxide derivatives. Furthermore, these compounds would be formed on aerosol particles as results of photochemical processes in atmosphere with attendance of sulfuric acid (or sulfur dioxide) or because of partial combustion in the car engines (Gao et al., 2004; Liggio et al., 2007; Surratt et al., 2007; Gao et al., 2006). As shown in Table 2, the major CHOS molecular series present in group A1 contain 1 sulfur and 3 or 4 oxygens corresponding to the following general chemical formulas $C_xH_yO_3S$ and $C_xH_yO_4S$.

In addition, Kendrick mass defect (KMD) plot of CHOS molecular series present in group A1 exhibits common class of compounds with identical KMD and equal DBE values (Fig. 4). The linear horizontal block of dots in KMD plot represent series of homologues where each dot differs in its molecular composition by counts of $CH_2$-groups. For methylene-specific Kendrick mass analysis, the conversion factor of the IUPAC molecular mass to the Kendrick mass (KM) is 14.00000/14.01565 = 0.998883 (Schmitt-Kopplin et al., 2012) and can be expressed by the equation:

$$KM(CH_2) = \text{mass (IUPAC)} \times 14.00000/14.01565 = \text{mass (IUPAC)} \times 0.998883.$$

Then, the nominal KM is defined as the integer mass, and the KMD is the difference between the Kendrick mass and the nominal Kendrick mass:

$$KMD(CH_2) = \text{nominal } KM(CH_2) - KM(CH_2).$$

There are 4 series of $C_xH_yO_3S$ homologues with DBE from 0 to 3 and 3 series of $C_xH_yO_4S$ homologues with DBE from 0 to 2. This fact is likely associated with similar origin of hydrocarbons being the precursors of sulfonated and sulfate esters. Other compounds from CHOS group represent individual dots on plot, so it's difficult to predict their natures and sources. All CHOS molecular series contain only one sulfur atom which excludes oligomerization processes in SOA possibly due to low temperatures and photochemical activity in winter season (Kalberer et al., 2004).

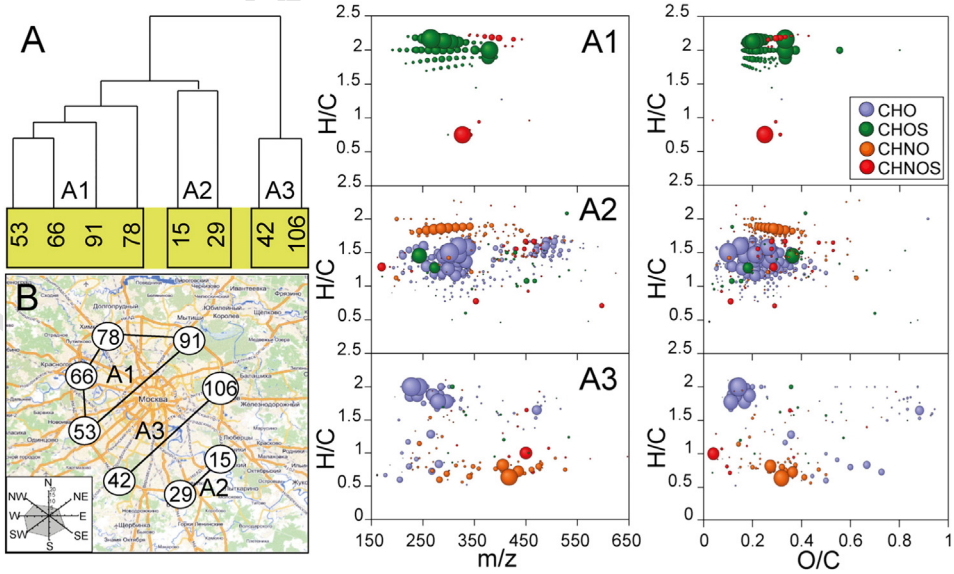


**Fig. 2.** Comparative analysis of the FT-ICR-MS data of the eight snow samples. (A) Clustering diagram based of the similarity values between the spectra of the eight snow samples using Pearson correlation. (B) Sampling location of the eight snow samples. (A1), (A2) and (A3) represent the H/C versus $m/z$ (middle) and H/C versus O/C van Krevelen plots of CHO (blue), CHNO (orange), CHOS (green) and CHONS (red) molecular series with high abundance in each group. Bubbles represent the relative mass peak intensity. (For interpretation of the references to color in this figure legend, the reader is referred to the web version of this article.)

Please cite this article as: Mazur, D.M., et al., High field FT-ICR mass spectrometry for molecular characterization of snow board from Moscow regions, Sci Total Environ (2015), http://dx.doi.org/10.1016/j.scitotenv.2016.02.178

**Table 2**
Calculated z-series and the double bond equivalent for $C_nH_{2n+z}O_3$ and $C_nH_{2n+z}SO_4$ compounds found with high abundance in group A1 (see also Fig. 4).

| Average mass (deprotonated) | C | H | O | S | O:C | H:C | DBE | Z | Formulas (neutral) |
|---|---|---|---|---|---|---|---|---|---|
| 221.12169 | 10 | 21 | 3 | 1 | 0.30 | 2.20 | 0 | 2 | $C_{10}H_{22}O_3S_1$ |
| 235.13733 | 11 | 23 | 3 | 1 | 0.27 | 2.18 | 0 | 2 | $C_{11}H_{24}O_3S_1$ |
| 249.15299 | 12 | 25 | 3 | 1 | 0.25 | 2.17 | 0 | 2 | $C_{12}H_{26}O_3S_1$ |
| 263.16863 | 13 | 27 | 3 | 1 | 0.23 | 2.15 | 0 | 2 | $C_{13}H_{28}O_3S_1$ |
| 277.18429 | 14 | 29 | 3 | 1 | 0.21 | 2.14 | 0 | 2 | $C_{14}H_{30}O_3S_1$ |
| 291.19993 | 15 | 31 | 3 | 1 | 0.20 | 2.13 | 0 | 2 | $C_{15}H_{32}O_3S_1$ |
| 305.21560 | 16 | 33 | 3 | 1 | 0.19 | 2.13 | 0 | 2 | $C_{16}H_{34}O_3S_1$ |
| 319.23123 | 17 | 35 | 3 | 1 | 0.18 | 2.12 | 0 | 2 | $C_{17}H_{36}O_3S_1$ |
| 333.24690 | 18 | 37 | 3 | 1 | 0.17 | 2.11 | 0 | 2 | $C_{18}H_{38}O_3S_1$ |
| 347.26254 | 19 | 39 | 3 | 1 | 0.16 | 2.11 | 0 | 2 | $C_{19}H_{40}O_3S_1$ |
| 191.07474 | 8 | 15 | 3 | 1 | 0.38 | 2.00 | 1 | 0 | $C_8H_{16}O_3S_1$ |
| 205.09040 | 9 | 17 | 3 | 1 | 0.33 | 2.00 | 1 | 0 | $C_9H_{18}O_3S_1$ |
| 219.10604 | 10 | 19 | 3 | 1 | 0.30 | 2.00 | 1 | 0 | $C_{10}H_{20}O_3S_1$ |
| 233.12170 | 11 | 21 | 3 | 1 | 0.27 | 2.00 | 1 | 0 | $C_{11}H_{22}O_3S_1$ |
| 247.13734 | 12 | 23 | 3 | 1 | 0.25 | 2.00 | 1 | 0 | $C_{12}H_{24}O_3S_1$ |
| 261.15299 | 13 | 25 | 3 | 1 | 0.23 | 2.00 | 1 | 0 | $C_{13}H_{26}O_3S_1$ |
| 275.16864 | 14 | 27 | 3 | 1 | 0.21 | 2.00 | 1 | 0 | $C_{14}H_{28}O_3S_1$ |
| 289.18429 | 15 | 29 | 3 | 1 | 0.20 | 2.00 | 1 | 0 | $C_{15}H_{30}O_3S_1$ |
| 303.19995 | 16 | 31 | 3 | 1 | 0.19 | 2.00 | 1 | 0 | $C_{16}H_{32}O_3S_1$ |
| 317.21558 | 17 | 33 | 3 | 1 | 0.18 | 2.00 | 1 | 0 | $C_{17}H_{34}O_3S_1$ |
| 331.23124 | 18 | 35 | 3 | 1 | 0.17 | 2.00 | 1 | 0 | $C_{18}H_{36}O_3S_1$ |
| 345.24691 | 19 | 37 | 3 | 1 | 0.16 | 2.00 | 1 | 0 | $C_{19}H_{38}O_3S_1$ |
| 217.09039 | 10 | 17 | 3 | 1 | 0.30 | 1.80 | 2 | −2 | $C_{10}H_{18}O_3S_1$ |
| 231.10605 | 11 | 19 | 3 | 1 | 0.27 | 1.82 | 2 | −2 | $C_{11}H_{20}O_3S_1$ |
| 245.12168 | 12 | 21 | 3 | 1 | 0.25 | 1.83 | 2 | −2 | $C_{12}H_{22}O_3S_1$ |
| 259.13733 | 13 | 23 | 3 | 1 | 0.23 | 1.85 | 2 | −2 | $C_{13}H_{24}O_3S_1$ |
| 273.15299 | 14 | 25 | 3 | 1 | 0.21 | 1.86 | 2 | −2 | $C_{14}H_{26}O_3S_1$ |
| 287.16864 | 15 | 27 | 3 | 1 | 0.20 | 1.87 | 2 | −2 | $C_{15}H_{28}O_3S1$ |
| 301.18428 | 16 | 29 | 3 | 1 | 0.19 | 1.88 | 2 | −2 | $C_{16}H_{30}O_3S_1$ |
| 315.19994 | 17 | 31 | 3 | 1 | 0.18 | 1.88 | 2 | −2 | $C_{17}H_{32}O_3S_1$ |
| 329.21560 | 18 | 33 | 3 | 1 | 0.17 | 1.89 | 2 | −2 | $C_{18}H_{34}O_3S_1$ |
| 257.12170 | 13 | 21 | 3 | 1 | 0.23 | 1.69 | 3 | −4 | $C_{13}H_{22}O_3S_1$ |
| 271.13734 | 14 | 23 | 3 | 1 | 0.21 | 1.71 | 3 | −4 | $C_{14}H_{24}O_3S_1$ |
| 285.15302 | 15 | 25 | 3 | 1 | 0.20 | 1.73 | 3 | −4 | $C_{15}H_{26}O_3S_1$ |
| 299.16866 | 16 | 27 | 3 | 1 | 0.19 | 1.75 | 3 | −4 | $C_{16}H_{28}O_3S_1$ |
| 313.18427 | 17 | 29 | 3 | 1 | 0.18 | 1.76 | 3 | −4 | $C_{17}H_{30}O_3S_1$ |
| 327.19993 | 18 | 31 | 3 | 1 | 0.17 | 1.78 | 3 | −4 | $C_{18}H_{32}O_3S_1$ |
| 341.21555 | 19 | 33 | 3 | 1 | 0.16 | 1.79 | 3 | −4 | $C_{19}H_{34}O_3S_1$ |
| 265.14791 | 12 | 25 | 4 | 1 | 0.33 | 2.17 | 0 | 2 | $C_{12}H_{26}O_4S_1$ |
| 321.21051 | 16 | 33 | 4 | 1 | 0.25 | 2.13 | 0 | 2 | $C_{16}H_{34}O_4S_1$ |
| 335.22614 | 17 | 35 | 4 | 1 | 0.24 | 2.12 | 0 | 2 | $C_{17}H_{36}O_4S_1$ |
| 349.24182 | 18 | 37 | 4 | 1 | 0.22 | 2.11 | 0 | 2 | $C_{18}H_{38}O_4S_1$ |
| 363.25746 | 19 | 39 | 4 | 1 | 0.21 | 2.11 | 0 | 2 | $C_{19}H_{40}O_4S_1$ |
| 277.14791 | 13 | 25 | 4 | 1 | 0.31 | 2.00 | 1 | 0 | $C_{13}H_{26}O_4S_1$ |
| 291.16355 | 14 | 27 | 4 | 1 | 0.29 | 2.00 | 1 | 0 | $C_{14}H_{28}O_4S_1$ |
| 305.17919 | 15 | 29 | 4 | 1 | 0.27 | 2.00 | 1 | 0 | $C_{15}H_{30}O_4S_1$ |
| 319.19486 | 16 | 31 | 4 | 1 | 0.25 | 2.00 | 1 | 0 | $C_{16}H_{32}O_4S_1$ |
| 333.21049 | 17 | 33 | 4 | 1 | 0.24 | 2.00 | 1 | 0 | $C_{17}H_{34}O_4S_1$ |
| 347.22616 | 18 | 35 | 4 | 1 | 0.22 | 2.00 | 1 | 0 | $C_{18}H_{36}O_4S_1$ |
| 361.24181 | 19 | 37 | 4 | 1 | 0.21 | 2.00 | 1 | 0 | $C_{19}H_{38}O_4S_1$ |
| 375.25749 | 20 | 39 | 4 | 1 | 0.20 | 2.00 | 1 | 0 | $C_{20}H_{40}O_4S_1$ |
| 289.14791 | 14 | 25 | 4 | 1 | 0.29 | 1.86 | 2 | −2 | $C_{14}H_{26}O_4S_1$ |
| 303.16354 | 15 | 27 | 4 | 1 | 0.27 | 1.87 | 2 | −2 | $C_{15}H_{28}O_4S_1$ |
| 317.17918 | 16 | 29 | 4 | 1 | 0.25 | 1.88 | 2 | −2 | $C_{16}H_{30}O_4S_1$ |
| 331.19481 | 17 | 31 | 4 | 1 | 0.24 | 1.88 | 2 | −2 | $C_{17}H_{32}O_4S_1$ |
| 345.21051 | 18 | 33 | 4 | 1 | 0.22 | 1.89 | 2 | −2 | $C_{18}H_{34}O_4S_1$ |
| 301.14789 | 15 | 25 | 4 | 1 | 0.27 | 1.73 | 3 | −4 | $C_{15}H_{26}O_4S_1$ |
| 315.16355 | 16 | 27 | 4 | 1 | 0.25 | 1.75 | 3 | −4 | $C_{16}H_{28}O_4S_1$ |

Accordingly, the CHNOS molecular series in group A1 have different elemental ratios and they are much less abundant than the CHOS molecular series. This fact reflects the various sources of formation of these molecular series. In addition, the KMD plot showed a homologous series of CHNOS compounds with the following general chemical formula $C_nH_{2n+3}NO_5S_2$ (n = 13–17, 19). Taking in consideration only the number of oxygen atoms in this chemical formula, we could assume that nitrogen is in its reduced form and is likely amino group. Furthermore, these types of compounds may consequently or simultaneously form from hydrocarbons with attendance of ammonia, sulfur dioxide or sulfuric acid (O'Brien et al., 2013).

### 3.3.2. Group A2

Group A2 showed large proportion of CHO molecular series mainly positioned in van Krevelen plot in the ranges 1–1.75 of H/C ratio and 0.05–0.5 of O/C ratio (Fig. 2, A2). Along with this, a proportion of specific CHNO and few of CHOS and CHNOS molecular series are also present in this group of samples. Even CHO molecular series are positioned in specific area in van Krevelen plot, the KMD plot did not showed any trend regarding homologous series of compounds. This tendency reflects the fact that this class of molecular series is too various. However, the complexity of CHO compounds was described using plot of DBE and OSc versus number of carbon respectively (Fig. 3, A2). The most abundant compounds are positioned in 2 areas with 15–20 and 30 carbon atoms. OSc of these compounds varies from −0.5 to −1.5 and DBE from 4 to 9. Number of oxygen atoms in these molecular formulas varies from 5 to 9 with mean value −6.3 atoms of oxygen per molecule. Thus, compounds with these chemical characteristics are mainly associated with various compound classes (i.e., biogenic and anthropogenic aerosols, aged aerosols, and biomass burning organic aerosols (Kroll et al., 2011)). Namely they could represent oxidized unsaturated aliphatic and aromatic hydrocarbons.

As shown in Fig. 2A2, the major CHNO molecular series present in group A2 are shown in van Krevelen plot in the ranges H/C ≥ 1.5 ratio and O/C ratio between 0.15 and 0.45. Thus, the KMD plot of CHNO molecular series resulted in fairly scattered dots, but with one specific homologous series of compounds with the following common chemical formula $C_nH_{2n-2}N_2O_4$ (Fig. 4B). In general, most of the CHNO compounds are associated with nitro-compounds which are particularly formed in polluted air during day and night with attendance of $NO_x$ and $NO_3$ radical-initiated reactions in the presence of alkenes, respectively (Day et al., 2010). For instance, the chemical formula $C_nH_{2n-2}N_2O_4$ with DBE equal to 3 is apparently characteristic of naphthenes or alkenes with 2 nitro groups. By considering all other CHNO molecular series, it should be mentioned that the most abundant compounds have DBE between 3 and 5 with 1 or 2 nitrogen atoms. The mean DBE value for this type of compounds is about 5 with mean number of oxygen atoms around 5. As reported previously, we assume that these compounds include hydroxynitrates, dihydroxynitrates, carbonylnitrates, hydroperoxynitrates, as well as alkyl nitrites, nitrates and nitro compounds (Day et al., 2010).

Accordingly, the CHOS molecular series in group A2 differs in number of oxygen and sulfur atoms as well as DBE values. Based upon on KMD analysis, there is no homologous series among them. Aromatic and highly unsaturated aliphatic sulfur esters with H/C below 1.5 are the most abundant compounds in this group. In this group, there are few specific CHNOS molecular series but they do not show any regular correlation and therefore are of no particular interest in this investigation.

### 3.3.3. Group A3

As shown in Fig. 2, group A3 shows specific distribution of the CHO, CHNO, and CHNOS molecular series. Unlike the groups A1 and A2, CHO molecular series in group A3 are positioned in 3 distinct regions in van Krevelen plot (Fig. 2A3). Thus, the first region of CHO molecular series has high H/C ratio (H/C > 1.6), low O/C ratio (O/C < 0.2), DBE values between 1 and 5, and average carbon oxidation state between −1.5 and −2. The number of oxygen atoms varies between 1 and 7. This group mostly relates to hydrocarbon-like organic aerosols (Kroll et al., 2011). The $O_2$ and $O_3$ oxygen class of compounds in this region covering the DBE range of 1–4 and number of carbon 14–20 were found in relatively high abundance. The $O_2$ class of compounds with DBE equal to 1 mainly consists of carboxylic fatty acids or so-called naphthenic acids (Table 3, Fig. 5). These naphthenic acids which are mainly cycloaliphatic carboxylic acids have mainly carbon values between 10 and 16 and higher values of DBE (McKee et al., 2014). In relation, the $O_3$ class of compounds in this region arises mainly due to the oxidation processes of the $O_2$ class of compounds. Furthermore, these two classes of

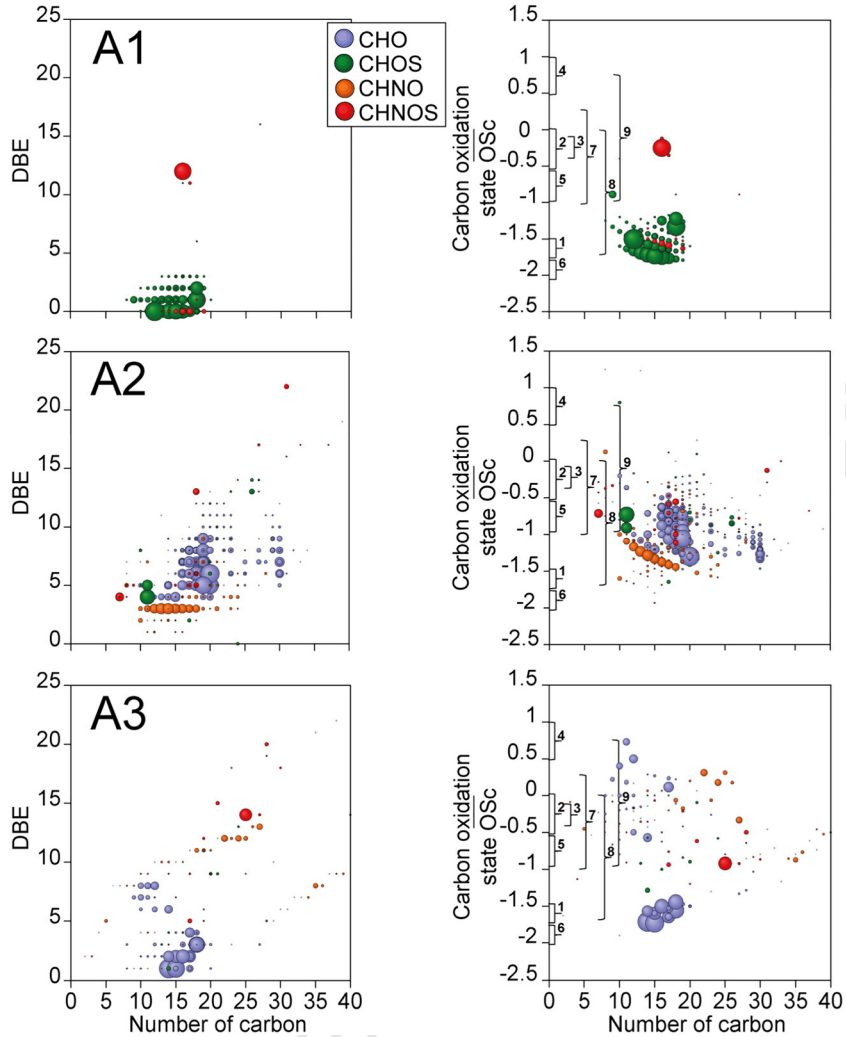


**Fig. 3.** DBE versus number of carbon and carbon oxidation state of CHO (blue), CHNO (orange), CHOS (green) and CHONS (red) molecular series with high abundance in A1, A2, and A3 groups. Bubbles represent the relative mass peak intensity. Overlays of compound classes designate organic aerosol classes for carbon oxidation state as: (1) hydrocarbon-like organic aerosol (HOA), (2) semi-volatile oxygenated organic aerosol (SV OOA), (3) humic-like substances (HULIS), (4) low volatility oxygenated organic aerosol (LV-OOA), (5) water soluble organic carbon (WSOC), (6) vehicle exhaust, (7) biogenic aerosol, (8) anthropogenic, and (9) aged aerosol and biomass burning organic aerosol (BBOA) (Kroll et al., 2011, Cottrell et al., 2013). (For interpretation of the references to color in this figure legend, the reader is referred to the web version of this article.)

Q5 compounds are widely discussed in petroleomics elsewhere (Clemente
Q6 and Fedorak, 2005, Rowland et al., 2011, Headley et al. 2011).

In relation, the second region in group A3 includes also CHO molecular series with high ratios of H/C (>1.5) and O/C (>0.75) (Fig. 2A3). These high ratios of H/C and O/C could emphasize carbohydrates like compounds as well as their derivatives. These compounds are typically phytochemicals which possibly introduced into snow from plants processes. The third region of CHO molecular series could also be representative of aromatic phytochemicals with rather high number of oxygen atoms (O/C > 0.5) and low H/C ratio (H/C < 1). Often such chemical compositions belong to various flavones, flavonoids and structurally related compounds. So, the last two CHO molecular series are apparently not from anthropogenic air pollutants, and therefore they can be excluded from consideration.

In addition, most of CHNO molecular series are positioned in aromatic area with H/C < 1 and O/C ratio between 0.4 and 0.2 (Fig. 2, A3). In addition, the iso abundance plot of DBE versus number of carbon atoms for this molecular series is shown in Fig. 6. The number of nitrogen atoms in formulas varies from 1 to 3 and the number of oxygen atoms from 2 to 9. The $N_1$ and $N_2$ nitrogen classes of compounds were spread over DBE ranges of (2–13 and 5–17) and carbon number (11–19 and 12–26), respectively. Thus, the highest relative abundance of $N_1$ class of compounds was at DBE values of 9 and 12. Accordingly, these are most likely compounds with neutral nitrogen mainly carbazoles, benzocarbazoles and dibenzocarbazoles (Hughey et al. Q7
2002, 2004) (Fig. 6). Furthermore, highly unsaturated compounds with DBE > 10 were observed for $N_2$ nitrogen class of compounds (Fig. 6). It has been reported that $N_2$ class of compounds with DBE of 17 likely have two fused carbazole cores (Hughey et al. 2002, 2004). Q8
We also assumed that these classes of compounds could be related to nitro-derivatives of polycyclic aromatic hydrocarbons (PAH). However, it is still challenging to assume structurally type of compounds that could be attributed to each assigned molecular formulas since no distinction between positional and optical isomers is possible.

### 3.4. Potential sources

Moscow is a large industrial center with lots of power plants, factories and facilities. There are dozens of factories inside the city and in the nearest surroundings: oil refinery, paper mills, foundries, chemical plants, polymeric factories, coal factory, rubber producing factories, etc. Moreover, there are 4 waste incineration plants in Moscow and

Please cite this article as: Mazur, D.M., et al., High field FT-ICR mass spectrometry for molecular characterization of snow board from Moscow regions, Sci Total Environ (2015), http://dx.doi.org/10.1016/j.scitotenv.2016.02.178

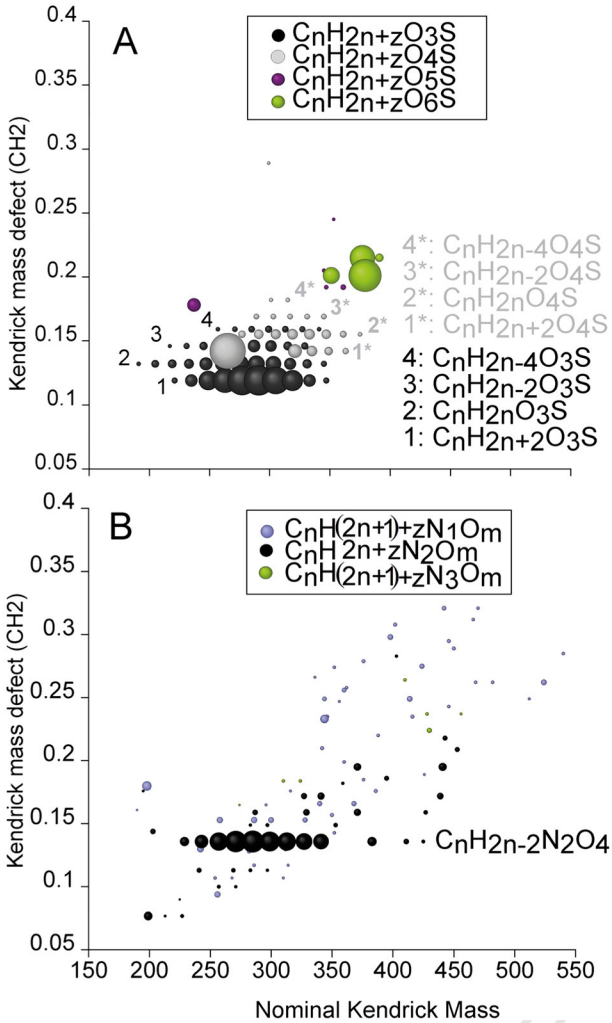


**Fig. 4.** (A) Kendrick mass defect versus nominal Kendrick mass of z-series distribution for $C_nH_{2n+z}O_3S$, $C_nH_{2n+z}O_4S$, $C_nH_{2n+z}O_5S$ and $C_nH_{2n+z}O_6S$ compounds in group A1 (see Fig. 2). (B) Kendrick mass defect versus nominal Kendrick mass of z-series distribution for $C_nH_{(2n+1)+z}N_1O_m$, $C_nH_{2n+z}N_2O_m$ and $C_nH_{(2n+1)+z}N_3O_m$ compounds in group A2 (see Fig. 2).

nearest surroundings. Traffic should be also considered as the main source of air pollution. Only in Moscow city more than 3.8 million cars are registered and about 3 million of cars are registered in Moscow

**Table 3**
Calculated z-series and the double bond equivalent of the compounds $C_nH_{2n+z}O_2$ and $C_nH_{2n+z}O_3$ (namely carboxylic acids) found with high abundance in group A3.

| Average mass (deprotonated) | C | C | O | O:C | H:C | DBE | z | Formulas (neutral) |
|---|---|---|---|---|---|---|---|---|
| 227.20166 | 14 | 27 | 2 | 0.14 | 2.00 | 1 | 0 | $C_{14}H_{28}O_2$ |
| 241.21731 | 15 | 29 | 2 | 0.13 | 2.00 | 1 | 0 | $C_{15}H_{30}O_2$ |
| 225.18600 | 14 | 25 | 2 | 0.14 | 1.86 | 2 | −2 | $C_{14}H_{26}O_2$ |
| 239.20166 | 15 | 27 | 2 | 0.13 | 1.87 | 2 | −2 | $C_{15}H_{28}O_2$ |
| 267.23296 | 17 | 31 | 2 | 0.12 | 1.88 | 2 | −2 | $C_{17}H_{32}O_2$ |
| 251.20166 | 16 | 27 | 2 | 0.13 | 1.75 | 3 | −4 | $C_{16}H_{28}O_2$ |
| 265.21731 | 17 | 29 | 2 | 0.12 | 1.76 | 3 | −4 | $C_{17}H_{30}O_2$ |
| 279.23297 | 18 | 31 | 2 | 0.11 | 1.78 | 3 | −4 | $C_{18}H_{32}O_2$ |
| 277.21732 | 18 | 29 | 2 | 0.11 | 1.67 | 4 | −6 | $C_{18}H_{30}O_2$ |
| 257.21221 | 15 | 29 | 3 | 0.20 | 2.00 | 1 | 0 | $C_{15}H_{30}O_3$ |
| 285.24353 | 17 | 33 | 3 | 0.18 | 2.00 | 1 | 0 | $C_{17}H_{34}O_3$ |
| 269.21222 | 16 | 29 | 3 | 0.19 | 1.88 | 2 | −2 | $C_{16}H_{30}O_3$ |
| 283.22787 | 17 | 31 | 3 | 0.18 | 1.88 | 2 | −2 | $C_{17}H_{32}O_3$ |
| 295.22787 | 18 | 31 | 3 | 0.17 | 1.78 | 3 | −4 | $C_{18}H_{32}O_3$ |
| 309.24352 | 19 | 33 | 3 | 0.16 | 1.79 | 3 | −4 | $C_{19}H_{34}O_3$ |
| 323.25918 | 20 | 35 | 3 | 0.15 | 1.80 | 3 | −4 | $C_{20}H_{36}O_3$ |

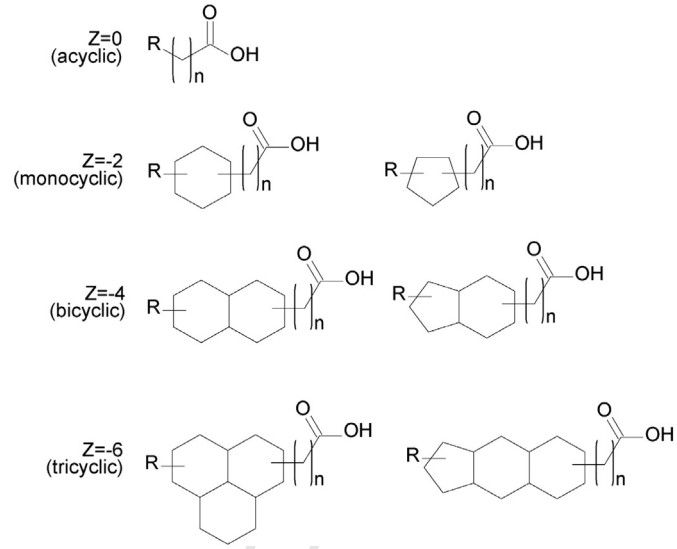


**Fig. 5.** Proposed structures of the hydrocarbon cores for compounds $C_nH_{2n+z}O_2$ (namely naphthenic acids) and $C_nH_{2n+z}O_3$ (oxy-naphthenic acids) found with high abundance in group A3. R could be various aliphatic substituents.

region. All these sources yield massive amounts of chemicals responsible for air pollution. Also the presence of sulfonated and nitrated type of compounds in aerosols becomes obvious due to presence of $SO_2$ and $NO_x$ in atmosphere.

## 4. Conclusions

High field FT-ICR mass spectrometry analysis of the eight snow samples from Moscow city allowed a clustering into 3 groups. The statistical processing showed good correlation with the wind directions. Group A1 clearly stands out with specific homologues of CHOS molecular compositions with different DBE values. It seems that all North-West segment of Moscow differs by higher amount of $SO_2$ emissions in atmosphere that can transform into reactive sulfuric acid by photochemical reactions including oxidation of hydrocarbons and sulfonation. As a result higher amounts of sulfur esters appear in aerosols and then in snow matrix. Group A2, located in the South-East part of Moscow, contains considerable amount of oxidized hydrocarbons of

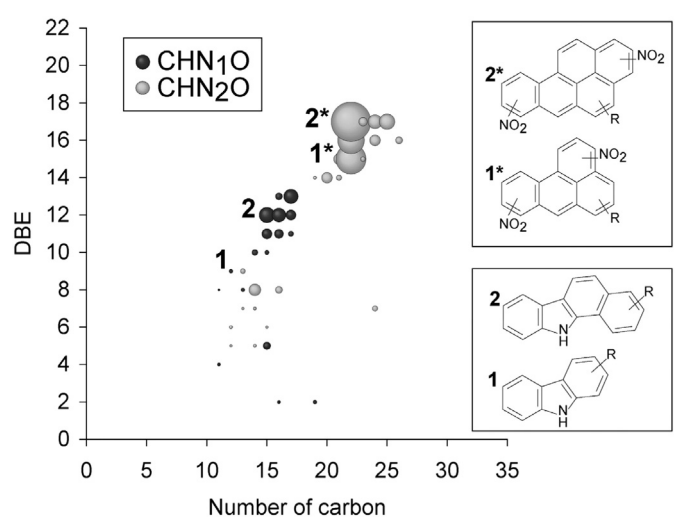


**Fig. 6.** DBE versus number of carbon atoms in CHN1O and CHN2O molecular series with high abundance in group A3 (see also Fig. 2). Bubbles represent the relative mass peak intensity. Suggested structures cores correspond to the DBE values of 9, 12, 15 and 17 respectively. The proposed core structures are examples of many other plausible structures of the assigned molecular formulas.



Please cite this article as: Mazur, D.M., et al., High field FT-ICR mass spectrometry for molecular characterization of snow board from Moscow regions, Sci Total Environ (2015), http://dx.doi.org/10.1016/j.scitotenv.2016.02.178

different natures (aromatic, aliphatic, alicyclic). Those compounds including $O_2$ and $O_3$ classes are mainly formed during atmospheric oxidation. This could be the effect of large emissions of hydrocarbons from traffic, oil refinery which is situated exactly in this region, and power plants. Another family of compounds specific for this region is CHNO with the following molecular formula $C_nH_{2n-2}N_2O_4$. Similarly to CHOS, CHNO compounds are formed during 2 oxidation processes including $NO_x$ and $NO_3$ radical. Thus, emissions of $NO_x$ in this part of the city are obviously higher. Group A3 is rich in CHO type of compounds with high H/C and low O/C ratios which is characteristic of aliphatic acids, aldehydes and ketones. In addition group A3 contains CHNO type of compounds probably nitro derivatives of PAH. Such a non-targeted mapping of the distribution of different substances is the first step for the development of new strategies in air quality control, defining priority pollutants for further monitoring of Moscow's air environment.

## References


Antony, R., Grannas, A.M., Willoughby, A.S., Sleighter, R.L., Thamban, M., Hatcher, P.G., 2014. Origin and sources of dissolved organic matter in snow on the East Antarctic ice sheet. Environ. Sci. Technol. 48, 6151–6159.

Clemente, J.S., Fedorak, PH.M., 2005. A review of the occurrence, analyses, toxicity and biodegradation of naphthenic acids. Chemosphere 60, 585–600.

Cottrell, B.A., Gonsior, M., Isabelle, L.M., Luo, W., Perraud, V., McIntire, T.M., Pankow, J.F., Schmitt-Kopplin, Ph., Cooper, W.J., Simpson, A.J., 2013. A regional study of the seasonal variation in the molecular composition of rainwater. Atmos. Environ. 77, 588–597.

Day, D.A., Liu, S., Russell, L.M., Ziemann, P.J., 2010. Organonitrate group concentrations in submicron particles with high nitrate and organic fractions in coastal southern California. Atmos. Environ. 44, 1970–1979.

Fries, E., Starokozhev, E., Haunold, W., Jaeschke, W., Mitra, S.K., Borrmann, S., 2007. Laboratory studies on the uptake of aromatic hydrocarbons by ice crystals during vapor depositional crystal growth. Atmos. Environ. 41, 6156–6166.

Fries, E., Sieg, K., Püttmann, W., Jaeschke, W., Winterhalter, R., Williams, J., Moortgat, G.K., 2008. Benzene, alkylated benzenes, chlorinated hydrocarbons and monoterpenes in snow/ice at Jungfraujoch (46.6°N, 8.0°E) during LACE 4 and 5. Sci. Total Environ. 391, 269–277.

Gao, S., Keywood, M., Ng, N.L., Surratt, J.D., Varutbangkul, V., Bahreini, R., Flagan, R.C., Seinfeld, J.H., 2004. Low-molecular-weight and oligomeric components in secondary organic aerosol from the ozonolysis of cycloalkenes and α-pinene. J. Phys. Chem. 108, 10147–10164.

Gao, S., Surratt, J.D., Knipping, J.D., Edgerton, E.M., Shahgholi, E.S., Seinfeld, M., 2006. Characterization of polar organic components in fine aerosols in the southeastern United States: identity, origin, and evolution. J. Geophys. Res. 111, D14314.

Headley, J.V., Armstrong, S.A., Peru, K.M., Mikula, R.J., Germida, J.J., Mapolelo, M.M., Rodgers, R.P., Marshall, A.G., 2010. Ultrahigh-resolution mass spectrometry of simulated runoff from treated oil sands mature fine tailings. Rapid Commun. Mass Spectrom. 24, 2400–2406.

Headley, J.V., Peru, K.M., Barrow, M.P., Derrick, P.J., 2007. Characterization of naphthenic acids from athabasca oil sands using electrospray ionization: the significant influence of solvents. Anal. Chem. 79, 6222–6229.

Hertkorn, N., Frommberger, M., Schmitt-Kopplin, Ph., Witt, M., Koch, B., Perdue, E.M., 2008. Natural organic matter and the event horizon of mass spectrometry. Anal. Chem. 80, 8908–8919.

Hertkorn, N., Meringer, M., Gugisch, R., Ruecker, C., Frommberger, M., Perdue, E.M., Witt, M., Schmitt-Kopplin, Ph., 2007. High-precision frequency measurements: indispensable tools at the core of the molecular-level analysis of complex systems. Anal. Bioanal. Chem. 389, 1311–1327.

Kalberer, M., Paulsen, D., Sax, M., Steinbacher, M., Dommen, J., Fisseha, R., Prevot, A., Frankevich, V., Zenobi, R., Baltensperger, U., 2004. Identification of polymers as major components of atmospheric organic aerosols. Science 303, 1659–1662.

Kroll, J.H., Donahue, N.M., Jimenez, J.L., Kessler, S.H., Canagaratna, M.R., Wilson, K.R., Altieri, K.E., Mazzoleni, L.R., Wozniak, A.S., Bluhm, H., Mysak, E.R., Smith, J.D., Kolb, C.E., Worsnop, D.R., 2011. Carbon oxidation state as a metric for describing the chemistry of atmospheric organic aerosol. Nat. Chem. 3, 133–139.

Laniewski, K., Borern, H., Grimvall, A., 1998. Identification of volatile and extractable chloroorganics in rain and snow. Environ. Sci. Technol. 32, 3935–3940.

Lebedev, A.T., 2013. Environmental mass spectrometry. Annu. Rev. Anal. Chem. 6, 163–189.

Lebedev, A.T., Mazur, D.M., Polyakova, O., Hanninen, O., 2015. Snow samples as markers of air pollution in mass spectrometry analysis. Environ. Indic. 515-541.

Lebedev, A.T., Polyakova, O.V., Karakhanova, N., Petrosyan, V., Renzoni, A., 1998. The contamination of birds with organic pollutants in the Lake Baikal region. Sci. Total Environ. 212, 153–162.

Lebedev, A.T., Polyakova, O.V., Mazur, D.M., Artaev, V.B., 2013. The benefits of high resolution mass spectrometry in environmental analysis. Analyst 138, 6946–6953.

Lebedev, A.T., Sinikova, N.A., Nikolaeva, S.N., Poliakova, O.V., Khrushcheva, M., Pozdnyakov, S., 2003. Metals and organic pollutants in snow surrounding an iron factory. Toxicol. Environ. Chem. 75, 181–194.

Liggio, J., Li, S.M., Brooks, J.R., Mihele, C., 2007. Direct polymerization of isoprene and α-pinene on acidic aerosols. Geophys. Res. Lett. 34, L05814.

McKee, R.H., North, C.M., Podhasky, P., Charlap, J.H., Kuhl, A., 2014. Toxicological assessment of refined naphthenic acids in a repeated dose/developmental toxicity screening test. Int. J. Toxicol. 33, 168S–180S.

Nizkorodov, S.A., Laskin, J., Laskin, A., 2011. Molecular chemistry of organic aerosols through the application of high resolution mass spectrometry. Phys. Chem. Chem. Phys. 13, 3612–3629.

O'Brien, R.E., Nguyen, T.B., Laskin, A., Laskin, J., Hayes, P.L., Liu, S., Jimenez, J.L., Russell, L.M., Nizkorodov, S.A., Goldstein, A.H., 2013. Probing molecular associations of field-collected and laboratory generated SOA with nano-DESI high-resolution mass spectrometry. J. Geophys. Res. Atmos. 118, 1042–1051.

Ortiz, X., Jobst, K.J., Reiner, E.J., Backus, S.M., Peru, K.M., McMartin, W., O'Sullivan, G., Taguchi, V.Y., Headley, J.V., 2014. Characterization of naphthenic acids by gas chromatography-Fourier transform ion cyclotron resonance mass spectrometry. Anal. Chem. 86, 7666–7673.

Poliakova, O.V., Lebedev, A.T., Hanninen, O., 2003. Organic pollutants in snow of urban and rural Russia and Finland. Environ. Chem. Lett. 1, 107–112.

Polyakova, O.V., Mazur, D.M., Seregina, I.F., Bolshov, M.A., Lebedev, A.T., 2012. Estimation of contamination of atmosphere of Moscow in winter. J. Anal. Chem. 67, 1039–1049 (Original Russian version in Mass-spektrometria (Rus). 2012, 9, 5–15).

Rowland, S.J., Scarlett, A.G., Jones, D., West, C.E., Frank, R.A., 2011. Diamonds in the rough: identification of individual naphthenic acids in oil sands process water. Environ. Sci. Technol. 45, 3154–3159.

Schmitt-Kopplin, Ph., Gabelica, Z., Gougeon, R.D., Fekete, A., Kanawati, B., Harir, M., Gebefuegi, I., Eckel, G., Hertkorn, N., 2010b. High molecular diversity of extraterrestrial organic matter in Murchison meteorite revealed 40 years after its fall. Proc. Natl. Acad. Sci. U. S. A. 107, 2763–2768.

Schmitt-Kopplin, Ph., Gelencse'r, A., Dabek-Zlotorzynska, E., Kiss, G., Hertkorn, N., Harir, M., Hong, Y., Gebefugi, I., 2010a. Analysis of the unresolved organic fraction in atmospheric aerosols with ultrahigh-resolution mass spectrometry and nuclear magnetic resonance spectroscopy: organosulfates as photochemical smog constituents. Anal. Chem. 82, 8017–8026.

Schmitt-Kopplin, P.H., Harir, M., Tziotis, D., Gabelica, Z., Hertkorn, N., 2012. Ultrahigh resolution Fourier transform ion cyclotron (FTICR) mass spectrometry for the analysis of natural organic matter from various environmental systems Chapter 19 In: Lebedev, Albert (Ed.), Comprehensive Environmental Mass Spectrometry 2012. ILM Publications, pp. 443–459.

Sieg, K., Fries, E., Püttmann, W., 2008. Analysis of benzene, toluene, ethylbenzene, xylenes and *n*-aldehydes in melted snow water via solid-phase dynamic extraction combined with gas chromatography/mass spectrometry. J. Chromatogr A. 1178, 178–186.

Surratt, J.D., Lewandowski, M., Offenberg, J.H., Jaoui, M., Kleindienst, T.E., Edney, E.O., Seinfeld, J.H., 2007. Effect of acidity on secondary organic aerosol formation from isoprene. Environ. Sci. Technol. 41, 5363–5369.

Van Krevelen, D.W., 1950. Graphical-statistical method for the study of structure and reaction processes of coal. Fuel 29, 269–284.

Yassine, M.M., Dabek-Zlotorzynska, E., Harir, M., Schmitt-Kopplin, Ph., 2012. Identification of weak and strong organic acids in atmospheric aerosols by capillary electrophoresis-mass spectrometry and ultrahigh resolution Fourier transform ion cyclotron resonance mass spectrometry. Anal. Chem. 84, 6586–6594.

Yassine, M.M., Harir, M., Dabek-Zlotorzynska, E., Schmitt-Kopplin, Ph., 2014. Structural characterization of organic aerosol using Fourier transform ion cyclotron resonance mass spectrometry: aromaticity equivalent approach. Rapid Commun. Mass Spectrom. 28, 2445–2454.

Zhao, Y., Hallar, A.G., Mazzoleni, L.R., 2013. Atmospheric organic matter in clouds: exact masses and molecular formula identification using ultrahigh-resolution FT-ICR mass spectrometry. Atmos. Chem. Phys. 13, 12343–12362.

Zoccolillo, L., Amendola, L., Cafaro, C., Insogna, S., 2007. Volatile chlorinated hydrocarbons in Antarctic superficial snow sampled during Italian ITASE expeditions. Chemosphere 67, 1897–1903.




Please cite this article as: Mazur, D.M., et al., High field FT-ICR mass spectrometry for molecular characterization of snow board from Moscow regions, Sci Total Environ (2015), http://dx.doi.org/10.1016/j.scitotenv.2016.02.178